Numerical studies of a 36-site *kagomé* antiferromagnet

P. W. Leung
*Supercomputer Computations Research Institute, Florida State University, Tallahassee, Florida 32306-4052 and Physics Department, The Hong Kong University of Science and Technology, Clear Water Bay, Hong Kong**

Veit Elser
Laboratory of Atomic and Solid State Physics, Cornell University, Ithaca, New York 14853-2501
(Received 2 September 1992)

The ground-state wave function for the spin-$\frac{1}{2}$ quantum antiferromagnet on a 36-site *kagomé* structure is found by numerical diagonalization. Spin-spin correlations and spin gaps indicate that the ground state of this system does not possess magnetic order. The spin-Peierls order is studied using a four-spin correlation function. The short-range structure in this correlation function is found to be consistent with a simple dimer-liquid model. The spin-Peierls order, if it exists, must be quite small.

It has long been speculated that low-dimensional quantum spin-$\frac{1}{2}$ antiferromagnets may have spin-disordered ground states.[1] Through various approaches, it is well established that the spin-$\frac{1}{2}$ Heisenberg antiferromagnet (HAF) on a square lattice, with Hamiltonian

$$\mathcal{H} = \sum_{\langle ij \rangle} \mathbf{S}_i \cdot \mathbf{S}_j, \tag{1}$$

has a magnetically ordered ground state.[2] Disordered ground states are more likely to be found in frustrated systems with large quantum fluctuations, i.e., small spin S and low coordination number. The HAF on the *kagomé* structure is a very good candidate because it is both frustrated and has a low coordination number. Classical spins on the *kagomé* structure are just as frustrated as spins on a triangular lattice but have a lower coordination number. Moreover, ground states for classical spins on the *kagomé* structure have a local degeneracy whereas the degeneracy on the triangular lattice is only the trivial global one.

Several independent approaches have concluded that the spin-$\frac{1}{2}$ *kagomé* HAF has a spin-disordered ground state.[3–7] The absence of a simple three-sublattice magnetic ordering has been convincingly demonstrated by the high-order perturbation theory treatment of Singh and Huse.[5] Unfortunately, this approach does not tell us anything obvious about the nature of the ground state in the range of parameters that includes the true HAF. Various exotic ground states have been proposed for the spin-$\frac{1}{2}$ *kagomé* HAF.[6–9] In particular, large-N expansions predict a ground state with spin-Peierls order for the group SU(N) (Ref. 6) and a spin liquid for the group Sp($N/2$).[7] To test these predictions for the case $N = 2$ a numerical technique can be used. Unfortunately, quantum Monte Carlo methods break down due to the problem associated with the fermion sign. Exact diagonalizations have so far been restricted to small systems up to 21 sites only.[3,4,10] Using finite-size scaling up to 18 sites, Chalker and Eastmond[10] conclude that the ground state of the *kagomé* HAF either has no or very weak spin-Peierls order. However, we caution that the smallest unit cell of the spin-Peierls solid of Marston and Zeng[6] (MZ) has 18 sites. Smaller systems cannot accommodate the kind of ordering they proposed. Furthermore, even the 18-site system still has the problem of having rings of four sites wrapping around it — this becoming the dominant mode of resonance among near-neighbor singlet (valence-bond) states. The smallest system having even number of sites that is free of these spurious resonances (and also able to accommodate the proposed spin-Peierls states) has 36 sites. In this paper, we present exact diagonalization results for the 36-site *kagomé* HAF.

We use the Lanczos algorithm[11] to calculate the ground state of the 36-site *kagomé* HAF. Using all possible point group symmetries for zero momentum as well as spin reflection, the $S^z_{\text{total}} = 0$ sector still has 31 527 894 states. The ground-state energy per spin is $E_0/N = -0.438\,377$. Since we have no reason to believe the ground state has long-range magnetic order, it makes no sense to use spin-wave theory together with results from smaller systems to extrapolate to the thermodynamic limit. In fact, the 36-site system may be the smallest that is representative of the true ground state. We note that the trend toward higher energy with system size is consistent with the elimination of spurious energy-lowering wraparound resonances. In Table I we tabulate the spin-spin correlations. Also shown are the spin-spin correlations for the HAF on a 36-site triangular lattice.[12] It is obvious that the spin-spin correlations of the *kagomé* HAF fall off much faster than its triangular analogue. In Fig. 1 we plot $|\langle S^z_0 S^z_n \rangle|$ versus r. Except for the last point at $r = 4$, all data points seem to be bounded by an exponentially decaying function with correlation length less than 1. This is strong evidence that the ground state is magnetically disordered.

Another way to show the absence of magnetic order is to look at the spin gap Δ, defined as the excitation energy of the lowest energy state with a higher $\mathbf{S}_{\text{total}}$ than the ground state. We were not able to calculate the spin gap

TABLE I. Spin-spin correlations $\langle S_0^z S_n^z \rangle$ at various separations r in the 36-site *kagomé* and triangular HAF. The near-neighbor spacing is unity. For the *kagomé* structure, the reference site 0 is site 26 in Fig. 2, and n refers to the site in the same figure. Results for the triangular HAF are from Ref. 12.

n	r	*kagomé*	Triangular
27	1	−0.07306	−0.06226
15	$\sqrt{3}$	0.00386	0.05115
34	2	0.01758	−0.01826
14	2	−0.00300	
21	$\sqrt{7}$	−0.00159	−0.02214
3	3	−0.00766	0.03787
32	$2\sqrt{3}$	0.00210	0.03914
6	$2\sqrt{3}$	0.00106	
7	$\sqrt{13}$	−0.00328	
22	4	0.00740	

for the 36-site *kagomé* HAF. The spin gaps of smaller systems are given in Table II. It appears that Δ approaches a value of $\sim \frac{1}{4}$ as $N \to \infty$. As in smaller lattices,[4] the 27-site *kagomé* HAF has many excited states between the ground state and the lowest quartet state. The first excited state is a doublet (same $\mathbf{S}_{\text{total}}$ as the ground state) with momentum $(\pi/3, \pi/3\sqrt{3})$ and excitation energy 0.001 51. Of these low-lying states, some may correspond to true singlet modes in the thermodynamic limit while the energies of others may collapse to the ground-state energy more rapidly and provide a signature of symmetry breaking.[13] We conclude that the apparent saturation of the spin gap in larger systems (up to 27 sites) is consistent with the absence of long-range magnetic order.

The most direct way of distinguishing spin-liquid from spin-Peierls order is to measure the dimer-dimer correlations, $\langle (\mathbf{S}_i \cdot \mathbf{S}_j)(\mathbf{S}_k \cdot \mathbf{S}_l) \rangle$, where spins i and j are near neighbors and distinct from near-neighbor spins k and

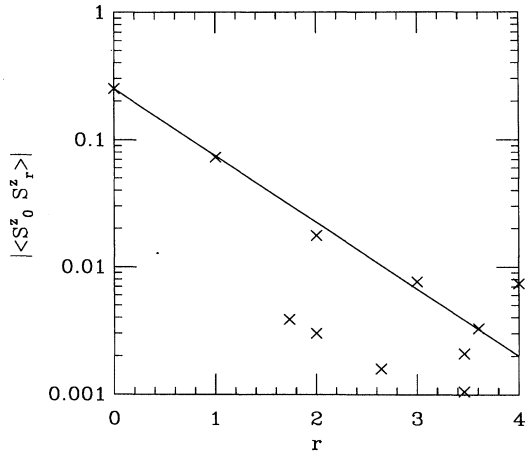

FIG. 1. Two spin correlations $\langle S_0^z S_n^z \rangle$ of the 36-site *kagomé* HAF. The straight line is a guide for the eye.

TABLE II. The size dependence of the spin gaps for the *kagomé* HAF. The discrepancies between some entries in this table and those in Table II of Ref. 3 stem from the fact that only zero momentum states were considered in the latter whereas all momentum states were examined in the present table.

N	Δ
12	0.38267
15	0.41880
18	0.28457
21	0.27864
27	0.26878

l. A liquidlike state would display short-range structure in this expectation value but would approach $\langle \mathbf{S}_i \cdot \mathbf{S}_j \rangle^2$ at large dimer separation. A spin-Peierls state, in contrast, would continue to show periodic oscillations reflecting the nonuniform value of $\langle \mathbf{S}_i \cdot \mathbf{S}_j \rangle$ in the presence of translational symmetry breaking. The expectation values $\langle (\mathbf{S}_i \cdot \mathbf{S}_j)(\mathbf{S}_k \cdot \mathbf{S}_l) \rangle$ for the 25 inequivalent dimer pairs of the 36-site system are given in Table III. (See Fig. 2 for the numbering of the sites.) The short-range structure is explained quite well by a simple near-neighbor valence-bond state[1] where each configuration carries the same weight. If the four-spin expectation value is calculated by including only terms that are diagonal in the configuration of valence bonds, then

$$\langle (\mathbf{S}_i \cdot \mathbf{S}_j)(\mathbf{S}_k \cdot \mathbf{S}_l) \rangle \approx (-3/4)^2 P_{(i,j)(k,l)}, \tag{2}$$

where $P_{(i,j)(k,l)}$ is the probability that bonds (i,j) and (k,l) are occupied by dimers. As in Fig. 2, the reference bond is (25,26). We see that $P_{(25,26)(k,l)}$ is clearly zero for $(k,l) = (34,35)$, since this would re-

TABLE III. Four spin correlations of the 25 inequivalent dimer pairs of the 36-site *kagomé* structure from exact diagonalization and the MZ spin-Peierls solid. See Fig. 2 for the numbering of the sites.

(k,l)	$C_{(25,26)(k,l)}$ (Exact results)	$C_{(25,26)(k,l)}$ (MZ model)	$\langle (\mathbf{S}_{25} \cdot \mathbf{S}_{26})(\mathbf{S}_k \cdot \mathbf{S}_l) \rangle$ (Exact results)
(5,6)	−0.00628	−0.03516	0.04177
(4,5)	0.00603	0.03516	0.05407
(3,4)	−0.00273	−0.02344	0.04531
(3,8)	0.00710	0.03516	0.05514
(4,8)	−0.00430	−0.01172	0.04374
(5,9)	0.00366	0.02344	0.05170
(9,14)	−0.00560	−0.02344	0.04245
(8,13)	0.00315	0.00000	0.05120
(8,12)	−0.00385	−0.02344	0.04420
(11,12)	−0.00016	−0.01172	0.04820
(12,13)	0.00010	0.01172	0.04814
(13,14)	0.00045	0.00000	0.04850
(14,15)	0.01221	0.01172	0.06025
(14,19)	−0.00113	0.01172	0.04692
(13,19)	0.00108	−0.01172	0.04912
(11,18)	−0.00419	−0.02344	0.04386
(18,22)	−0.00134	0.00000	0.04671
(19,24)	0.04337	0.03516	0.09141
(22,23)	−0.00214	−0.01172	0.04590
(23,24)	−0.01416	0.01172	0.03389
(23,29)	0.01322	0.00000	0.06127
(29,32)	−0.00646	0.03516	0.04159
(32,33)	0.01178	0.00000	0.05982
(34,35)	−0.06510	−0.03516	−0.01705
(1,33)	−0.01045	0.02344	0.03759

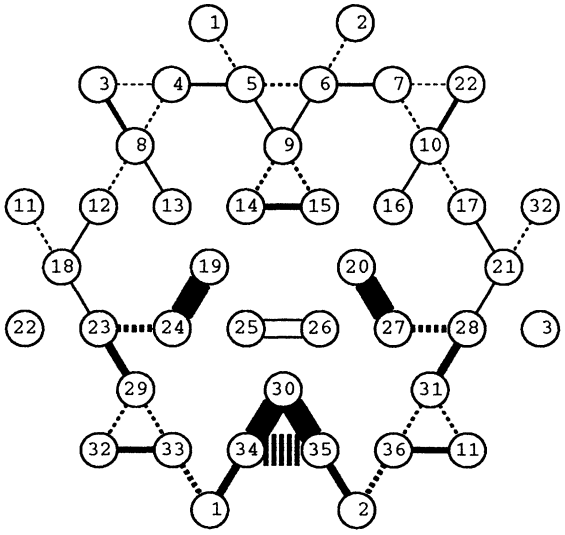

FIG. 2. Four spin correlations $C_{(i,j)(k,l)}$ of the 36-site *kagomé* HAF. The reference bond (25,26) is represented by a double line. The magnitude of $C_{(25,26)(k,l)}$ is proportional to the thickness of the line joining the pair of sites (k,l). The solid line means $C_{(25,26)(k,l)}$ is positive, and the broken line means $C_{(25,26)(k,l)}$ is negative.

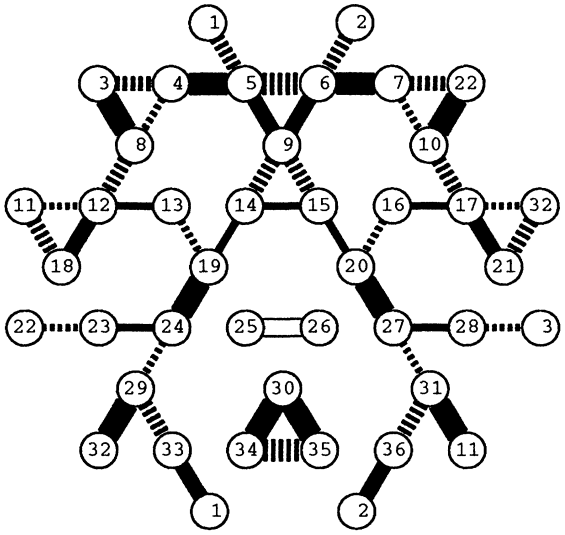

FIG. 3. Four spin correlations $C_{(i,j)(k,l)}$ of the spin-Peierls solid proposed in Ref. 6. Conventions are the same as in Fig. 2.

quire a spin to be unpaired. It can easily be shown[14] that $P_{(25,26)(k,l)} = 1/8$ for $(k,l) = (19,24)$ and other equivalent bond pairs, while $P_{(25,26)(k,l)} = 1/16$ for all other other bond pairs. This simple model thus predicts that all $\langle(\mathbf{S}_{25}\cdot\mathbf{S}_{26})(\mathbf{S}_k\cdot\mathbf{S}_l)\rangle$ are the same except for $(k,l) = (19,24)$ and (34,35), which have equal and opposite deflections of magnitude $(-3/4)^2(1/16) = 0.035$ from the rest. This is in fair agreement with the results in Table III, although the value 0.035 is a bit too small compared with the results in Table III.

To analyze the long-range structure of the four-spin correlations, we subtract a constant term from the expectation values,

$$C_{(i,j)(k,l)} = \langle(\mathbf{S}_i\cdot\mathbf{S}_j)(\mathbf{S}_k\cdot\mathbf{S}_l)\rangle - \langle\mathbf{S}_i\cdot\mathbf{S}_j\rangle^2. \quad (3)$$

Figure 2 shows the dimer-dimer correlations $C_{(i,j)(k,l)}$ for all dimer pairs of the 36-site *kagomé* structure. Positive correlations are represented by solid lines and negative correlations are represented by broken lines. The thickness of the lines is proportional to $C_{(i,j)(k,l)}$. The numerical values of $C_{(i,j)(k,l)}$ are tabulated in Table III. Using a simple model where $\langle(\mathbf{S}_i\cdot\mathbf{S}_j)(\mathbf{S}_k\cdot\mathbf{S}_l)\rangle = (-3/4)^2$ if both spin pairs (i,j) and (k,l) form dimers, and zero otherwise, we can construct the dimer-dimer correlations for the spin-Peierls solid proposed by MZ.[6] The constant term in Eq. (3) is given by

$$\langle\mathbf{S}_i\cdot\mathbf{S}_j\rangle = (3/4)f, \quad (4)$$

where $f = 1/4$ is the fraction of near-neighbor spin pairs that form dimers. For each hexagon with three dimers ("perfect hexagon") in the MZ spin-Peierls solid there are two resonating states corresponding to the two possible arrangements of the three dimers around the hexagon.[15] These resonating states are degenerate in the large-N limit. On the 36-site *kagomé* structure, there are two perfect hexagons, and hence four such resonating states. Figure 3 shows the dimer-dimer correlations $C_{(i,j)(k,l)}$ of the MZ spin-Peierls solid averaged over translations, lattice symmetries, and the four resonating states. The numerical values of $C_{(i,j)(k,l)}$ are also tabulated in Table III. We notice that the modulation of the dimer-dimer correlations for the more distant dimer pairs in Fig. 2 mostly agrees with the MZ spin-Peierls solid. Nevertheless, the amplitude of spin-Peierls order, if present, must be quite weak.

To conclude, we have calculated the ground-state wave function for the 36-site *kagomé* HAF using numerical diagonalization. From the spin-spin correlations and the energy gaps (of systems up to 27 sites), we conclude that the *kagomé* HAF does not have magnetic order. Our results for the dimer-dimer correlation function are clearly consistent with a dimerized state in its short-range properties and cannot rule out the possibility of a very weak spin-Peierls modulation amplitude in the ground state.

We thank Brad Marston for helpful discussions. V.E. was supported by the Sloan Foundation. The numerical diagonalizations were performed on the Thinking Machines Corporation Connection Machine CM-2 at the Florida State University Supercomputer Computations Research Institute (SCRI), which is partially funded by the U.S. Department of Energy through Contract No. DE-FC05-85ER25000.

*Present address.
[1]P. W. Anderson, Mater. Res. Bull. **8**, 153 (1973).
[2]E. Manousakis, Rev. Mod. Phys. **63**, 1 (1991), and references therein.
[3]C. Zeng and V. Elser, Phys. Rev. B **42**, 8436 (1990).
[4]C. C. Wan (unpublished).
[5]R. R. P. Singh and D. A. Huse, Phys. Rev. Lett. **68**, 1766 (1992).
[6]J. B. Marston and C. Zeng, J. Appl. Phys. **69**, 5962 (1991).
[7]S. Sachdev, Phys. Rev. B **45**, 12377 (1992).
[8]V. Elser, Phys. Rev. Lett. **62**, 2405 (1989).
[9]I. Ritchey, P. Coleman, and P. Chandra (unpublished).
[10]J. T. Chalker and J. F. G. Eastmond (unpublished).
[11]J. K. Cullum and R. A. Willoughby, *Lanczos Algorithms for Large Symmetric Eigenvalue Computations* (Birkhauser, Boston, 1985). For the implementation of the Lanczos algorithm on the Connection Machine CM-2, see P. W. Leung and P. E. Oppenheimer, Comput. Phys. (to be published).
[12]P. W. Leung and K. J. Runge, Phys. Rev. B (to be published).
[13]B. Bernu, C. Lhuillier, and L. Pierre, Phys. Rev. Lett. **69**, 2590 (1992).
[14]V. Elser and C. Zeng (unpublished).
[15]See Fig. 1(b) in Ref. 6.